ARCHIVES OF METALLURGY

Volume 45 2000 Issue 4

DMITRY SVIETLICHNYJ *

PROBLEMS OF MODELLING OF YIELD STRESS IN THE ON-LINE CONTROL OF HOT ROLLING PROCESSES

PROBLEMY MODELOWANIA NAPRĘŻENIA UPLASTYCZNIAJĄCEGO PRZY STEROWANIU W CZASIE RZECZYWISTYM PROCESEM WALCOWANIA NA GORĄCO

Model of the yield stress, applicable to the on-line control of hot steel plate rolling, is described in the paper. Developed model has a physical meaning. Three methods, based on an analysis of large number of experimental data, are applied for evaluation of coefficients in the model. These methods are approximation, optimisation and artificial neural network. Yield stress was not measured directly. It was determined from the roll force measurements, using inverse calculations of Sims equation. The results for three groups of steels (two carbon-manganese steels and one niobium steel), are presented in the publication. The adaptation technique is described in the paper, as well. Application of the adaptation technique allows for immediate reaction of the system on the changes of yield stress. Experimental validation of the model confirmed its good accuracy and usefulness for the on-line control of the hot plate rolling process.

W artykule opisano model naprężenia uplastyczniającego przystosowany do sterowania w czasie rzeczywistym walcowaniem blach grubych na gorąco. Opracowany model ma podstawy fizyczne. Trzy metody oparte o analizę dużej liczby danych doświadczalnych zastosowano do wyznaczania współczynników modelu. Tymi metodami są aproksymacja, optymalizacja oraz sztuczna sieć neuronową. Naprężenie uplastyczniające nie było wyznaczone bezpośrednio, lecz przez pomiary siły walcowania i obliczenia odwrotne z zastosowaniem metody Simsa. W pracy przedstawiono wyniki dla trzech grup stali (dwóch węglowomanganowych oraz jednej z dodatkiem niobu). Przedstawiono również metodę adaptacyjną. Zastosowanie adaptacji pozwala na szybkie reagowanie systemu na zmiany warunków walcowania a więc i na zmiany naprężenia uplastyczniającego. Weryfikacja modelu na danych doświadczalnych wskazuje na dobrą dokładność oraz możliwość implementacji go do systemów sterowania w czasie rzeczywistym procesem walcowania blach na gorąco.

* WYDZIAŁ METALURGII I INŻYNIERII MATERIAŁOWEJ, AKADEMIA GÓRNICZO-HUTNICZA, 30-059 KRAKÓW, AL. MICKIEWICZA 30

1. Introduction

On line control of the hot plate rolling process required fast and reliable models. Among several models, which are included in the control systems, the most important are those describing rolling force, temperature changes and profile of the plate. The rolling force model is usually based in the Sims formula [1] combined with the analytical description of the yield stress as a function of temperature, strain rate and strain. Problem of the selection of the stress-strain functions is widely discussed in the scientific literature (see for example [2]). Numerous papers dealing with the force models suitable for control systems for plate mills can be found, as well (see for example [3, 4]). Analysis of practical applications of roll force models shows that Sims' formula is frequently used. [5, 6, 7]. Possibility of an adaptation of the coefficients in the model is an interesting feature of the on-line systems. This feature is used in the current work for a development of a new yield stress model, which does not require experimental testing of the rolled material.

The objectives of the present work are twofold. The first is a critical analysis of various methods of development of the yield stress models suitable for the on-line control. The second is an attempt of employing the adaptation technique to the development of the yield stress models avoiding, or at least limiting, the experimental tests.

2. Rolling force model

2.1. General description

This model is a basis of the on-line control system. As it is mentioned in the introduction, among a number of possible methods the Sims' formula [1], described also in [4], is commonly used:

$$F = \bar{\sigma}_p l_d b Q, \tag{1}$$

where: $\bar{\sigma}_p$ — an average value of the yield stress, l_d — length of the arc of contact, b — width of the plate, Q — geometrical factor accounting for an influence of the plate thickness, reduction, roll radius and friction coefficient.

It is shown in [7] that simple equation (1) fully satisfies the requirements of the control systems. The average yield stress in (1) is calculated as:

$$\bar{\sigma}_p = \frac{1}{\varepsilon}\int_0^{\varepsilon} \sigma_p \, d\varepsilon, \tag{2}$$

where: σ_p — current value of the yield stress, which is usually determined from the plastometric tests and presented as a function of temperature, strain rate and strain.

Comparison of average and current values of the yield stress shows that both these parameters exhibit similar character of the correlation to the independent process parameters. It can be assumed with a good accuracy that the current value of the yield stress σ_p multiplied by a relevant coefficient can be introduced in the equation (1) [8]. This coefficient is constant for a given material.

2.2. Yield stress

An accuracy of the rolling force model depends mainly on the correctness of the description of the yield stress. Problem of the plastometric tests leading to the evaluation of the yield stress is investigated reasonably well [2, 9, 10]. Numerous examples of functions describing yield stress can be found in the scientific literature [9, 10], nevertheless, if often happens that these functions do not fit the experimental data properly in the whole range of the process parameters. In the temperatures above the recrystallisation stop temperatures the yield stress is affected by the competitive phenomena of hardening, recovery and recrystallisation, which are govern by the microstructural changes in the austenite [4, 10, 11, 12]. Due to these changes two types of the flow curves are possible. The first is characteristic for the materials in which hardening is compensated by recovery before the critical strain is achieved. The second type is typical for the materials, which exhibit dynamic recrystallisation. Hot rolled steels belong to the second group.

Analysis of the types of the stress- strain curves was performed in [2]. The following factors can be accounted for when modelling yield stress [9, 10]: i) microstructural phenomena, ii) changes of strain as a function of time, iii) orientation of main strain directions in the subsequent phases of the process. In consequence, five types of the stress strain functions are suggested in [2]:
Type I $\sigma_p = f(\varepsilon)$ accounts only for an influence of strain ε,
Type II $\sigma_p = f(\varepsilon, \varepsilon, T)$, accounts for an influence of temperature T, strain rate $\dot{\varepsilon}$ and strain ε,
Type III $\sigma_p = f(\varepsilon, \dot{\varepsilon}, T, \sigma_w)$, accounts additionally an influence of the internal state of the material σ_w,
Type IV $\sigma_p = f(\varepsilon, \dot{\varepsilon}, T, t)$ in which time t is an additional independent variable,
Type V composes functions accounting for changes of directions of the main strains during deformation.

Functions belonging to the type II are considered in the current work. In hot forming processes the yield stress is usually presented as a function of the chemical composition of steel, temperature, strain rate and strain. However, in the models developed for a particular rolling mill and advantage is taken from the fact that some of the parameters change in a narrow range what allows simplification of the function by omitting these parameters.

Continuity of the hot forming process is the main factor, which classifies this process with respect to the choice of the stress strain function. Plate rolling processes are sequential, what means that subsequent passes are separated by interpass times t_p. Length of these times decides how far an effect of one deformation is carried to the next pass. This effect is accounted for by calculation of so called retained strain.

Difficulties with the mathematical description of the yield stress function are connected with the wide range of changes of independent parameters. Significant simplification of the yield stress model is achieved when the strains below the peak strain are considered. This assumption is acceptable for plate rolling process in which dynamic recrystallisation rarely occurs. Thus, the following equation was considered in the present work [8, 14]:

$$\sigma = \exp\left(\frac{b}{T}\right)\left(\frac{\varepsilon}{0.2}\right)^m\left(\frac{\dot{\varepsilon}}{10}\right)^n. \tag{3}$$

In equation (3) *a*, *b*, *n* and *m* are the material constants, which are usually determined using approximation or optimisation technique [14].

2.3. Evaluation of material constants

Approximation is one of the methods, which allow evaluation of coefficients in equation (3). Function (3) is non-linear with respect to the independent variables. However, it can be linearised by calculating logarithm from both sides of equation (3):

$$\ln\sigma = \ln a + \frac{b}{T} + m\ln\left(\frac{\varepsilon}{0.2}\right) + n\ln\left(\frac{\dot{\varepsilon}}{10}\right). \tag{4}$$

In consequence, the relationship between $\ln(\sigma)$ and the parameters $\ln a$, b, m i n becomes linear and the following objective function can be formulated:

$$\delta = \sum_{i=1}^{k}\left[\ln a + \frac{b}{T_i} + m\ln\left(\frac{\varepsilon_i}{0.2}\right) + n\ln\left(\frac{\dot{\varepsilon}_i}{10}\right) - \ln\sigma_i\right]^2. \tag{5}$$

In equation (5) σ_i represents the yield stress calculated from the *i*-th experimental point. Typical approach to this problem uses experimental data obtained from plastometric tests. In the current approach the yield stress is determined from the rolling force measurements using inverse calculation of equation (1). This allows on-line adaptations of the yield stress model.

Application of the least squares method requires calculations of the derivatives of the objective function (5) with respect to the coefficients *a*, *b*, *m* and *n*:

$$\begin{cases} \dfrac{\partial \delta}{\partial b} = 2\sum\limits_{i=1}^{k}\left\{\dfrac{1}{T_i}\left[\dfrac{b}{T_i}+\ln a + m\ln\left(\dfrac{\varepsilon_i}{0.2}\right)+n\ln\left(\dfrac{\dot{\varepsilon}_i}{10}\right)-\ln\sigma_i\right]\right\} = 0 \\ \dfrac{\partial \delta}{\ln a} = 2\sum\limits_{i=1}^{k}\left[\dfrac{b}{T_i}+\ln a + m\ln\left(\dfrac{\varepsilon_i}{0.2}\right)+n\ln\left(\dfrac{\dot{\varepsilon}_i}{10}\right)-\ln\sigma_i\right] = 0 \\ \dfrac{\partial \delta}{\partial m} = 2\sum\limits_{i=1}^{k}\left\{\ln\left(\dfrac{\varepsilon_i}{0.2}\right)\left[\dfrac{b}{T_i}+\ln a + m\ln\left(\dfrac{\varepsilon_i}{0.2}\right)+n\ln\left(\dfrac{\dot{\varepsilon}_i}{10}\right)-\ln\sigma_i\right]\right\} = 0 \\ \dfrac{\partial \delta}{\partial n} = 2\sum\limits_{i=1}^{k}\left\{\ln\left(\dfrac{\dot{\varepsilon}_i}{10}\right)\left[\dfrac{b}{T_i}+\ln a + m\ln\left(\dfrac{\varepsilon_i}{0.2}\right)+n\ln\left(\dfrac{\dot{\varepsilon}_i}{10}\right)-\ln\sigma_i\right]\right\} = 0 \end{cases}, \tag{6}$$

Rearranging of equation (6) and introduction of the matrix notation yields:

$$\mathbf{Ax} = \mathbf{p}, \tag{7}$$

where:

$$\boldsymbol{A} = \begin{bmatrix} \sum \dfrac{1}{T_i^2} & \sum \dfrac{1}{T_i} & \sum \dfrac{1}{T_i}\ln\left(\dfrac{\varepsilon_i}{0.2}\right) & \sum \dfrac{1}{T_i}\ln\left(\dfrac{\dot{\varepsilon}_i}{10}\right) \\ \sum \dfrac{1}{T_i} & k & \sum \ln\left(\dfrac{\varepsilon_i}{0.2}\right) & \sum \ln\left(\dfrac{\dot{\varepsilon}_i}{10}\right) \\ \sum \dfrac{1}{T_i}\ln\left(\dfrac{\varepsilon_i}{0.2}\right) & \sum \ln\left(\dfrac{\varepsilon_i}{0.2}\right) & \sum \ln^2\left(\dfrac{\varepsilon_i}{0.2}\right) & \sum \ln\left(\dfrac{\varepsilon_i}{0.2}\right)\ln\left(\dfrac{\dot{\varepsilon}_i}{10}\right) \\ \sum \dfrac{1}{T_i}\ln\left(\dfrac{\dot{\varepsilon}_i}{10}\right) & \sum \ln\left(\dfrac{\dot{\varepsilon}_i}{10}\right) & \sum \ln\left(\dfrac{\varepsilon_i}{0.2}\right)\ln\left(\dfrac{\dot{\varepsilon}_i}{10}\right) & \sum \ln^2\left(\dfrac{\dot{\varepsilon}_i}{10}\right) \end{bmatrix},$$

$$\boldsymbol{x} = \begin{Bmatrix} b \\ \ln a \\ m \\ n \end{Bmatrix} \qquad \boldsymbol{p} = \begin{Bmatrix} \sum \dfrac{1}{T_i}\ln\sigma_i \\ \sum \ln\sigma_i \\ \sum \ln\left(\dfrac{\varepsilon_i}{0.2}\right)\ln\sigma_i \\ \sum \ln\left(\dfrac{\dot{\varepsilon}}{10}\right)\ln\sigma_i \end{Bmatrix}.$$

Coefficients *a*, *b*, *m* and *n* is equation (3) are calculated by solution of the set of linear equations (7). Approximation yields coefficients, which give minimum of the sum of squares of differences between logarithms of error in each measurement point. Better accuracy can be obtained using optimisation technique, which searches for a minimum of the error function:

$$E = \sum_{i=1}^{k} \left[a \exp\left(\frac{b}{T_i}\right) \left(\frac{\varepsilon_i}{0.2}\right)^m \left(\frac{\dot{\varepsilon}_i}{10}\right)^n - \sigma_i \right]^2 \tag{8}$$

with respect to the coefficients *a*, *b*, *m* and *n*. Gradient method was used to solve the problem. In this method changes of the unknowns in subsequent iterations are calculated as:

$$\mathbf{x}_j = \mathbf{x}_{j-1} - \Delta \mathbf{x}_j = \mathbf{x}_{j-1} - \boldsymbol{\eta}_j \mathbf{I} \frac{\partial E}{\partial x_j^T} \tag{9}$$

where: $\mathbf{x} = \{a, b, m, n\}^T$, $\boldsymbol{\eta}_j$ — vector of the step length for the *j*-th iteration, $\mathbf{I}$ — unity matrix. Influence of the unknowns on the error norm is determined by the partial derivatives in equation (9) given by:

$$\begin{aligned} \frac{\partial E}{\partial a} &= \frac{2}{a} \sum_{i=1}^{k} \sigma_{ji} (\sigma_{ji} - \sigma_i) \\ \frac{\partial E}{\partial b} &= 2 \sum_{i=1}^{k} \frac{1}{T_i} \sigma_{ji} (\sigma_{ji} - \sigma_i) \\ \frac{\partial E}{\partial m} &= 2 \sum_{i=1}^{k} \left\{ \ln\left(\frac{\varepsilon_i}{0.2}\right) \sigma_{ji} (\sigma_{ji} - \sigma_i) \right\} \\ \frac{\partial E}{\partial n} &= 2 \sum_{i=1}^{k} \left\{ \ln\left(\frac{\dot{\varepsilon}_i}{10}\right) \sigma_{ji} (\sigma_{ji} - \sigma_i) \right\} \end{aligned} \tag{10}$$

n

The tendency of stopping the procedure in local minima can be limited and the solution can be accelerated by an introduction of additional term in the equation describing increments of variables $\Delta \mathbf{x}$:

$$\Delta \mathbf{x}_j = \boldsymbol{\eta}_j \mathbf{I} \frac{\partial E}{\partial \mathbf{x}_j^T} + \mu \Delta \mathbf{x}_{j-1} \tag{11}$$

where: μ — coefficient accounting for an influence of the vector of increments $\Delta \mathbf{x}$ in the previous iteration. Additional improvement of the quality of optimisation is achieved by using variable vector of the length of steps $\boldsymbol{\eta}$. This length is increased when the error norm decreases noticeably comparing to the previous iteration. Change of the step length is calculated from the following equation:

$$\eta_{l,j+1} = \begin{cases} 1.2\,\eta_{lj} & \text{for } \left(\frac{\partial E}{\partial x_l}\right)_j \left(\frac{\partial E}{\partial x_l}\right)_{j-1} \geqslant 0 \\ 0.5\,\eta_{lj} & \text{for } \left(\frac{\partial E}{\partial x_l}\right)_j \left(\frac{\partial E}{\partial x_l}\right)_{j-1} < 0 \end{cases} \qquad l = 1,\ 2,\ 3,\ 4 \tag{12}$$

where: l — number of the unknown in the vector $\boldsymbol{x}$.

Both approximation and optimisation procedures have been applied to the evaluation of the coefficients a, b, m and n in the equation (3) for tested steels.

3. Application of artificial neural networks

When an application of approximation and optimisation techniques presents difficulties, the artificial neural network (ANN) becomes a useful tool in the description of the stress-strain curves. Training of the neural network follows the same principles as approximation. However, non-linearity of the neurone's transmission function results in higher flexibility of the ANN approach. The main fact, which distinguishes ANN from approximation, is a lack of equation, which relates output and input parameters. Neural network is a structure without precisely determined function describing physical phenomenon.

Analysis of data structure and network training performed in [15] has shown that the network configuration with three entry parameters (temperature, strain rate and strain) and with three neurones in the hidden layer allows obtaining good results. Increasing of the number of neurones does not improve the results noticeably, what is probably due to a significant scattering of the training data. Decrease of this scattering would probably require an introduction of additional neurones.

4. Results and Analysis

Table contains values of coefficients in equation (3) obtained from rolling force measurements by inverse calculations combined with approximation and optimisation techniques. Results of training of the artificial neural network are presented, as well. Three groups of steel grades were investigated. The first composed steels containing niobium (between 0.02 and 0.035% Nb). The next two groups compose carbon-manganese steels, distinguished by the carbon equivalent $C_{eq} = \mathrm{C} + \mathrm{Mn}/6$, where C and Mn represent contents of carbon and manganese, respectively. The investigation was performed within the temperature range 850–1150°C, strain rate range 1.9–30 s^{-1} and strain range 0.06–0.4. Analysis of the results shows reasonably good accuracy and an average square-root error was about 12–15 MPa. The difference between the two groups of carbon-manganese steels is negligible.

These observations gave a basis to connecting two groups of the carbon-manganese steels and the result is in the last row of table. All steels show small sensitivity to strains (*m* below 0.1) and only slightly higher sensitivity to strain rate (*n* about 0.18 – 0.26).

TABLE

Coefficients in equation (3) calculated using approximation and optimisation techniques as well as artificial neural network

Steel	Number of data points	Method	a	b	m	n	Average square-root error, MPa
Niobium	327	approximation	3.659	3845.8	0.0362	0.1814	14.6
		optimisation	3.998	3757.9	0.0109	0.1827	14.5
C-Mn I $C_{eq} = 0.2 - 0.27\%$	1415	approximation	10.913	2605.6	0.0843	0.2308	13.7
		optimisation	12.447	2477.8	0.0770	0.2405	13.6
C-Mn II $C_{eq} = 0.27 - 0.45\%$	728	approximation	9.640	2748.2	0.0838	0.2579	12.7
		optimisation	11.025	2618.2	0.0717	0.2584	12.7
C-Mn $C_{eq} = 0.2 - 0.45\%$	1922	approximation	10.377	2650.7	0.0838	0.2383	13.5
		optimisation	11.762	2527.4	0.0752	0.2467	13.4
		ANN	—	—	—	—	12.96

Relationship between basic stress $\sigma_T = a\exp(b/T)$ and temperature for three tested groups of steels is presented in Fig. 1. Thin lines with symbols represent results obtained from optimisation for three groups of steel. Relation predicted by the

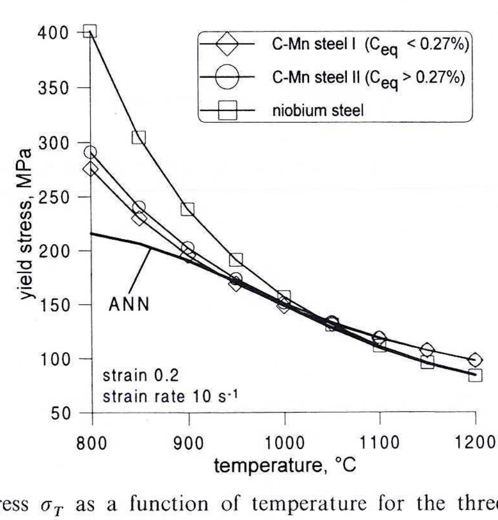

Fig. 1. Basic stress σ_T as a function of temperature for the three groups of steels

artificial neural network is presented, as well (thick line without symbols). Conclusion regarding a lack of difference between two groups of the carbon-manganese steels is confirmed. Distinct results were obtained for niobium steels, in particular at lower temperatures, where yield stress of niobium steels increases faster than that of carbon-manganese steels. Artificial neural network predicts smaller increase of the yield stress than equation (3).

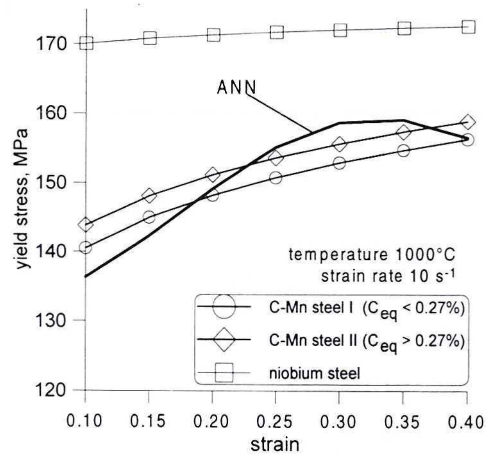

Fig. 2. Yield stress as a function of strain for the three groups of steels

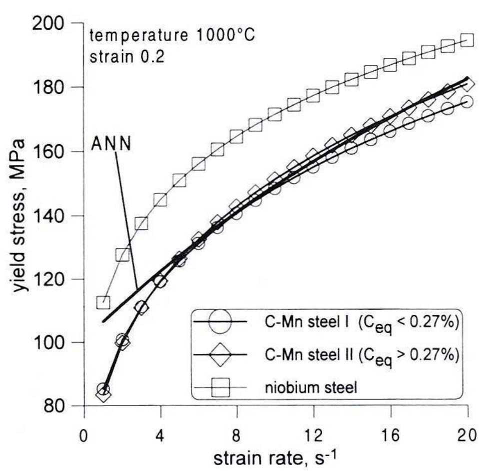

Fig. 3. Relation between the yield stress and the strain rate for the three groups of steels

Relations between yield stress and strain rate and strain are shown in Figs. 2 and 3. Character of plots for ANN questions ability of equation (3) to describe properly the yield stress within wide range of process parameters. However, the differences are not so large and model (3) can be considered acceptable.

Comparison of measured and predicted yield stress for niobium steels is shown in Fig. 4. Dotted line in this figure represents ideal correlation, when calculated force F_c is equal to the measured one F_m. Reasonably large scattering of results is observed in Fig. 4, what confirms values of errors in Table. This scattering allows suggestion that the consistency of the experimental data was low. Since a large number of the experimental results was examined, the statistical yields regression function which is close to the ideal one, what again confirms good predictive ability of equation (3) with coefficients given in Table.

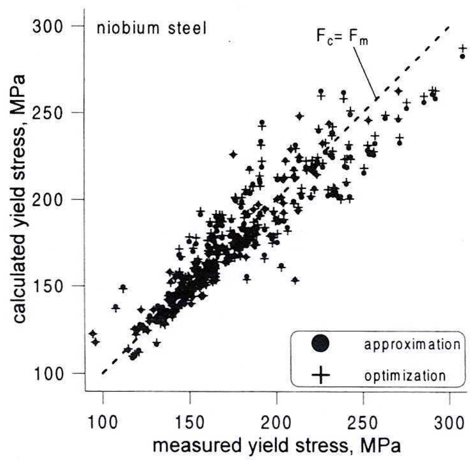

Fig. 4. Comparison between yield stress for niobium steels calculated from rolling force measured and calculated using equations with constants obtained from approximation and optimisation

Method of validation of the yield stress model is described in [8]. Physical basis is the main advantage of this model. Basic stress respesents yield stress determined as a function of temperature for the strain of 0.2 and the strain rate of 10 s^{-1}. Coeffieints m i n represent sensitivity of the yield stress to strain rate and strain, respectively. Influence of the chemical composition can be considered in two ways. The first assumes an introduction of separate curves for various carbon equivalents, as it is shown in Fig. 1. The second method introduces carbon equivalent as a variable into the model, as it is shown in [14]. This method causes an increase of the unknown variables to five.

6. Adaptivity of the model

Neural network yielded the best results. Since the trained neural network is very fast, its application in the on-line system does not present difficulties. However, training of the network requires large number of data and usually takes a long time. These long training times do not allow using for this process the same computer, which works in the control system. Thus, introduction of new data cannot have immediate impact on the network's predictions. Beyond this, a large database has to be maintained for each group of steels. All these fact allow to conclude that artificial neural network will not be efficient when often changes of steel grades take place and fast reaction of the system on these changes is required.

Since the flow stress is a feature of the material independent of time, the on-line changing of the model does not seem inevitable. It is due to two facts. Firstly, an introduction of new material requires new data. Secondly, measurement gauges always introduce a systematic error, which is not accounted for by the model.

The simplest on-line model uses the flow stress described by equation (3) with coefficients obtained from optimisation or approximation. All steels, which are rolled in the considered mill, can be grouped in several groups. Indeed, an application of the optimisation technique is not as time consuming as training of the ANN, nevertheless, it still has to be performed on a separate computer, which is not used in control. The fact that approximation does not require iterative procedure favours this method for the adaptive procedures.

Two approaches based on approximation are possible. The first uses contantly changing database followed by calculations of coefficients in equation (3) using the method described earlier. In this approach the computer memory and speed limit the size of the database. The second approach, which is pursued in the present work, allows obtaining similar effect with much smaller computer. The idea of this approach is based on using equation with on-line amendments of coefficients. Current average values of the considered parameters are calculated using the rule of digital filter:

$$x_{av,i} = (1-q)\,x_{av,i-1} + qx_i, \tag{13}$$

where: x_{av} — current, average value of the parameter x, i — iteration (pass) number, q — coefficient $(0 < q < 1)$.

Factor of proportionality this digital filter is equal 1. However, when value different than 1 can be used, the simplified equation is valid:

$$x_{av,i} = qx_{av,i-1} + x_i. \tag{14}$$

Care has to be taken of the fact that the same equation is used for each parameter. Efficiency of the suggested method has been validated. Developed computer program consists of:

- calculations of average values of all parameters in the 4×5 matrix;
- initial accumulation of average values;
- solution of the set of equations and evaluation of the coefficients in equation (3);
- calculation, using equation (3), of the yield stress for the next pass;
- comparison between measured and predicted yield stress (the points characterised by large discrepancy are discarded).

The data, which were previously used for optimisation and approximation, are here used for testing the adaptation technique. Since the available data could not be arranged according to the rolling sequence, two sets of data with random sequence have been prepared. Plots of average square root error and coefficients in equation (3) are presented in Figs 5–8, while corelation field is shown in Fig. 9. It should be emphasised that na average error for the considered cases is 13.08 MPa and 13.1 MPa. This error for approximation is 13.5 MPa and for optimisation 13.4 MPa, and is comparable with the error of the artificial neural network (13.0 MPa). During adaptation, all the coefficients in equation (3) change in a narrow range around the values calculated previously.

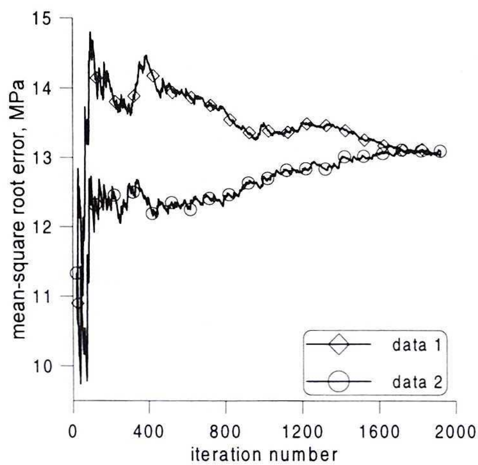

Fig. 5. Variations of the average square root error during adaptation

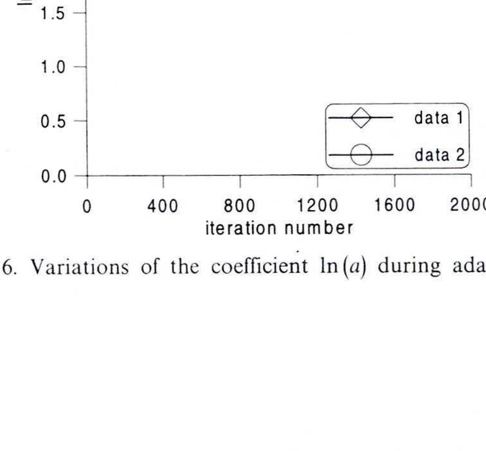

Fig. 6. Variations of the coefficient $\ln(a)$ during adaptation

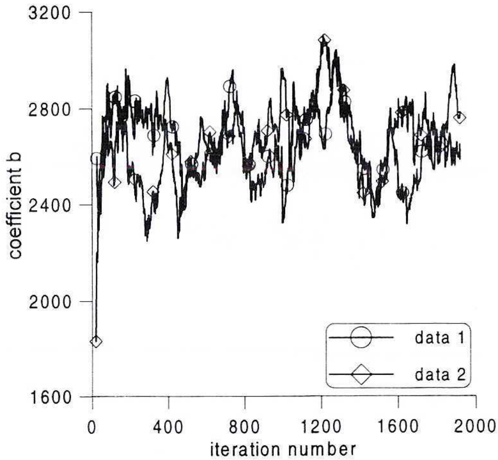

Fig. 7. Variations of the coefficient b during adaptation

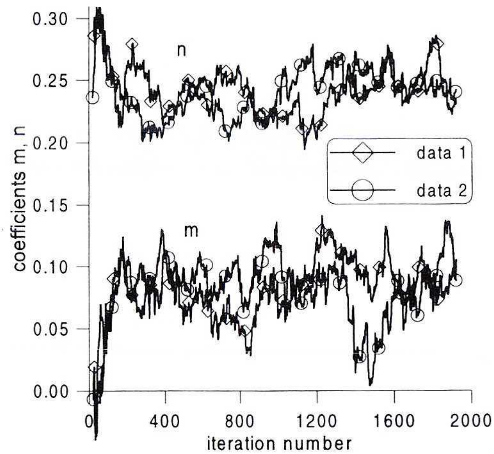

Fig. 8. Variations of the coefficients n, m during adaptation

The primary data set, with the data arranged according to the rolling schedule, is used in the second stage of adaptation. There are no limitations put on the values of measured temperatures, strains, strain rates and yield stresses. Undoubtedly, some of the wrong dara are in this set. Therefore, the points for which the difference between measured and calculated yield stress exceeded 30 MPa, were discarded. Results of calculations are shown in Figs 10–14. Thin line (data 4) shows calculations without discarding the erroneous points. Thick line (data 3) represents the results obtained for the selected data, with error within 30 MPa, calculated using the same algorithm.

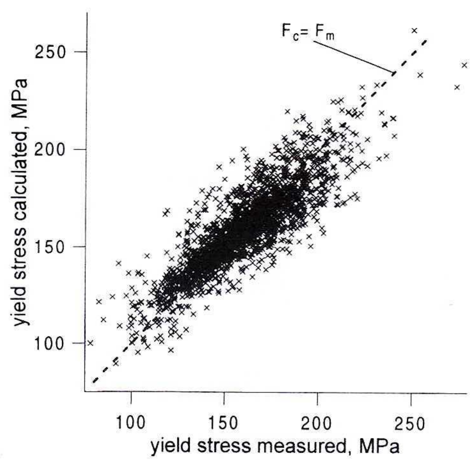

Fig. 9. Correlation between measured and calculated yield stress

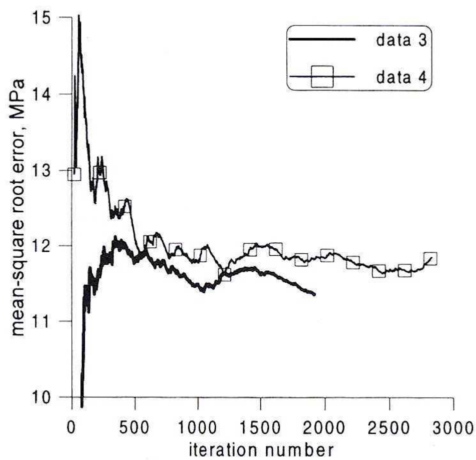

Fig. 10. Variations of the average square root during adaptation

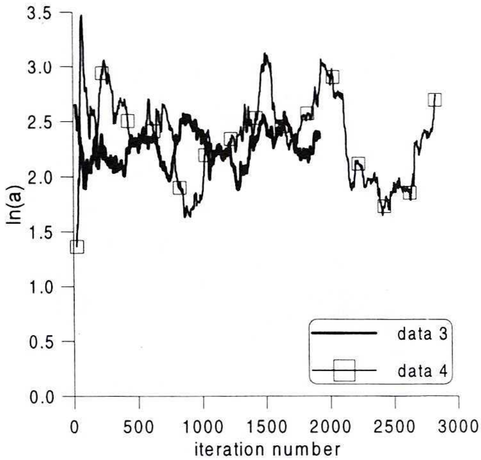

Fig. 11. Variations of the ln(a) during adaptation

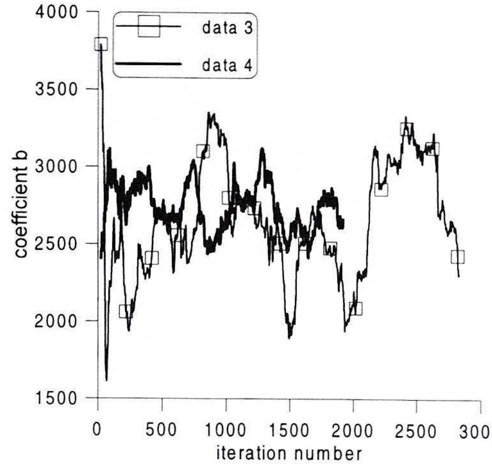

Fig. 12. Variations of the coefficients b during adaptation

Final average square root error is 11.85 and 11.36 MPa, which is even smaller than that for the ANN. Using all the data, including erroneous ones, leads to an increase of the total error. Further analysis shows that discarding the erroneous data is essential for the accuracy of the mode. Selection of the data can also be made on the basis of measurement of other parameters, for example temperatures. When the measure and calculated temperatures differ significantly, such a data point is rejected.

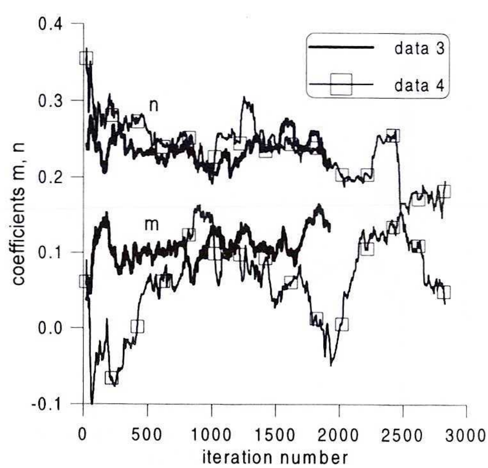

Fig. 13. Variations of the coefficients n, m during adaptation

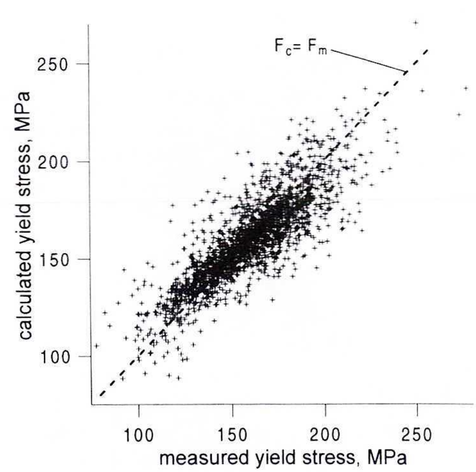

Fig. 14. Field of correlation between measured and calculated yield stress

7. Conclusions

Model of the yield stress, applicable to the on-line control of hot plate rolling, is described in the paper. Application of the approximation, optimisation and artificial neural network methods for evaluation of constants in the model yielded errors about 12–14 MPa. The efficiency of the model was significantly improved by an application of the adaptation technique, which is described in the paper, as well. This technique allows for immediate reaction of the system on the changes of yield stress. Experimental validation, based on the data monitored during normal work of the plate mill, confirmed good accuracy of the model and its usefulness for the on-line control of the hot plate rolling process.

Acknowledgements

Author thanks Kasa im. J. Mianowskiego (Poland) for founding his stay in Kraków

REFERENCES

[1] R. B. S i m s, The Calculation of Roll Force and Torque in Hot Rolling Mills, Proc. Inst. Mech. Eng., **168,** 191–200 (1954).

[2] F. G r o s m a n, Problems of Selection of a Flow Stress Functions for Computer Simulation of Manufacturing, Proc. CCME'97, eds, R. C i e s i e l s k i, B. C i s z e w s k i, J. G r o n o s t a j s k i, H. H a w r y l a k, J. K m i t a, S. K o b i e l a k, Wrocław, 67–76 (1997).

[3] W. L. R o b e r t s, Hot Rolling of Steel, Marcel Dekker, New York, 1983.

[4] J. G. L e n a r d, M. P i e t r z y k, L. C s e r, Mathematical and Physical Simulation of the Properties of Hot Rolled Products, Elsevier, Amsterdam, 1999.

[5] J. H. B e y n o n, C. M. S e l l a r s, Modelling Microstructure and its Effect during Multipass Hot Rolling, ISIJ Int., **32,** 359–367 (1992).

[6] P. D. H o d g s o n, D. C. C o l l i n s o n, 1990, The calculation of Hot Strength in Plate and Strip Rolling of Niobium Microalloyed Steels, Proc. Symp. Mathematical Modelling of Hot Rolling of Steel, (ed.), Yue, S., Hamilton, 239–250.

[7] D. S v i e t l i c h n y j, Z. U r b a n o w i c z, M. P i e t r z y k, Propozycja modelu projektowania schematu gniotów w walcowni blach grubych na gorąco, przystosowanego do pracy w systemie on-line, Proc. Conf. KomPlasTech'98, eds, M. P i e t r z y k, J. K u s i a k, A. P i e l a, Bukowina Tatrzańska, 1998, 209—218 (in Polish).

[8] D. S v i e t l i c h n y j, K. D u d e k, M. P i e t r z y k, Dobór modelu naprężenia uplastyczniającego do programu sterującego walcowaniem blach grubych w czasie rzeczywistym, Proc. Conf. PLAST'98, Ustroń, 1998, 1–8 (in Polish).

[9] E. H a d a s i k, A. P l o c h, I. S c h i n d l e r, B. M a c h u l e c, Wykorzystanie technik komputerowych do realizacji badań plastometrycznych, Proc. Conf. Zastosowanie komputerów w zakładach przetwórstwa metali, eds, J. K u s i a k, J. M a j t a, A. P i e l a, M. P i e t r z y k, Koninki, 1996, 41–47 (in Polish).

[10] J. K l i b e r, New Approaches in Describing Full Stress-Strain Curves, Proc. Formability'94, ed., Bartecek J., Ostrava, 77–83 (1994).

[11] C. M. S e l l a r s, Modelling Microstructural Development During Hot Rolling, Mat. Sci. Techn., **6,** 1072–1981 (1990).

[12] C. D e v a d a s, I. V. S a m a r a s e k e r a, E. B. H a w b o l t, The Thermal and Metallurgical State of Steel Strip during Hot Rolling: Part III. Microstructural Evolution, Metall. Trans., **22 A,** 335–349 (1991).

[13] R. Kuziak, Y.-W. Cheng, M. Głowacki, M. Pietrzyk, Modelling of the Microstructure and Mechanical Properties of Steels during Thermomechanical Processing, NIST Technical Report 1393, Boulder, 1997.

[14] D. Svietlichnyj, K. Dudek, Z. Urbanowicz, M. Pietrzyk, Wyznaczenie współczynników funkcji naprężenia uplastyczniającego dla programu sterującego walcowaniem blach grubych w czasie rzeczywistym, Proc. KomPlasTech'99, eds. A. Piela, F. Grosman, M. Pietrzyk, J. Kusiak, Szczyrk, 1999, 173–180 (in Polish).

[15] D. Svietlichnyj, Wybrane problemy przygotowania danych i uczenia sztucznych sieci neuronowych. Proc. 3rd Seminar NeuroMet'99, Kraków, 1999, 39–56 (in Polish).

REVIEWED BY: PROF. DR HAB. INŻ. MACIEJ PIETRZYK

Received: 20 September 2000.